JOURNAL OF VIROLOGY, Aug. 2003, p. 8237–8248 Vol. 77, No. 15
0022-538X/03/$08.00+0 DOI: 10.1128/JVI.77.15.8237–8248.2003

Cholesterol Depletion of Human Immunodeficiency Virus Type 1 and Simian Immunodeficiency Virus with β-Cyclodextrin Inactivates and Permeabilizes the Virions: Evidence for Virion-Associated Lipid Rafts

David R. M. Graham,[1] Elena Chertova,[2] Joanne M. Hilburn,[2] Larry O. Arthur,[2] and James E. K. Hildreth[1]*

The Leukocyte Immunochemistry Laboratory, Department of Pharmacology and Molecular Sciences, Johns Hopkins University School of Medicine, Baltimore, Maryland 21205,[1] and AIDS Vaccine Program, SAIC Frederick, NCI-Frederick, Frederick, Maryland 21702[2]

Received 2 October 2002/Accepted 7 May 2003

Recent evidence suggests that human immunodeficiency virus type 1 (HIV-1) particles assemble and bud selectively through areas in the plasma membrane of cells that are highly enriched with glycosylphosphatidylinositol-anchored proteins and cholesterol, called lipid rafts. Since cholesterol is required to maintain lipid raft structure and function, we proposed that virion-associated cholesterol removal with the compound 2-hydroxy-propyl-β-cyclodextrin (β-CD) might be disruptive to HIV-1 and simian immunodeficiency virus (SIV). We examined the effect of β-CD on the structure and infectivity of cell-free virions. We found that β-CD inactivated HIV-1 and SIV in a dose-dependent manner and permeabilized the viral membranes, resulting in the loss of mature Gag proteins (capsid, matrix, nucleocapsid, p1, and p6) without loss of the envelope glycoproteins. SIV also lost reverse transcriptase (RT), integrase (IN), and viral RNA. IN appeared to be only slightly diminished in HIV-1, and viral RNA, RT, matrix, and nucleocapsid proteins were retained in HIV-1 but to a much lesser degree. Host proteins located internally in the virus (actin, moesin, and ezrin) and membrane-associated host proteins (major histocompatibility complex classes I and II) remained associated with the treated virions. Electron microscopy revealed that under conditions that permeabilized the viruses, holes were present in the viral membranes and the viral core structure was perturbed. These data provide evidence that an intact viral membrane is required to maintain mature virion core integrity. Since the viruses were not fixed before β-CD treatment and intact virion particles were recovered, the data suggest that virions may possess a protein scaffold that can maintain overall structure despite disruptions in membrane integrity.

Lipid rafts are organized membrane microdomains that are enriched in sphingolipids, cholesterol, SRC family protein kinases, and glycosylphosphatidylinositol (GPI)-anchored proteins (7, 33; reviewed in reference 6). Lipid rafts are implicated as areas of the plasma membrane where human immunodeficiency virus type 1 (HIV-1) assembly and budding occurs in infected cells. Immunomicroscopy studies show that the HIV-1 core protein Gag and viral envelope proteins colocalize with lipid raft markers on the surface of infected cells (22, 37). Further, the GPI-anchored lipid raft markers CD55 and CD59 are incorporated into budding virions (12, 37), and virions exhibit high amounts of cholesterol, a finding consistent with the lipid composition of rafts (1). The initiation of budding is proposed to be driven by the multimerization of the myristylated and positively charged Gag polyprotein of the virus and its interactions with the inner leaflet of the plasma membrane (31, 37, 40). The association of the assembling virus with lipid rafts appears to result from the fact that myristylated Gag is found almost exclusively in lipid rafts (37). Viral budding is then dependent on interactions of host proteins with the PTAP motif in the P6 protein region, or the late domain, of the Gag polyprotein precursor (reviewed in reference 13).

Lipid rafts are also implicated as the area on the cell membrane where infection is established since, in both primary cells and cell lines, disruption of lipid raft regions by removing cholesterol with 2-hydroxy-propyl-β-cyclodextrin (β-CD) inhibits HIV-1-induced syncytium formation, reduces and interferes with coreceptor expression and function (27, 39, 47), and renders cells resistant to infection with CXCR4- and CCR5-specific HIV-1 strains of virus without losses in cell viability (29). Recent studies have showed that methyl-β-cyclodextrin depletion of virion-associated cholesterol reduced the buoyant density of viral particles (9) and almost completely eliminated virus infectivity, presumably by blocking virus fusion to target cells (9, 20, 57). The anti-HIV activity of β-CD has been evaluated in an animal model in which the compound was found to block vaginal transmission of cell-associated HIV-1 in a SCID-HuPBL mouse model with high efficacy (24).

In the present study, we have further examined the effect of β-CD on virus particle infectivity and integrity. Since the lipid composition of HIV-1 is high in cholesterol (1), a circumstance reminiscent of lipid rafts on cells, and since this lipid appears to be critical in sustaining their integrity, we sought to determine whether complete depletion of cholesterol by β-CD might reveal insights regarding the presence of lipid rafts on

* Corresponding author. Mailing address: Johns Hopkins School of Medicine, Department of Pharmacology and Molecular Sciences, 725 N. Wolfe St., 320A Physiology Bldg., Baltimore, MD 21205. Phone: (410) 955-3017. Fax: (410) 955-1894. E-mail: jhildret@jhmi.edu.

HIV-1 and SIV particles. We therefore examined the effect of β-CD on infectivity and virion integrity in both HIV-1_{MN}/H9 cl.4 (HIV-1) and SIV_{Mne}/Hut-78 cl.E11S (SIV), a virus that is well characterized and a candidate virus for use in vaccine studies in macaques (2, 3, 10, 51). Our results reveal that depletion of cholesterol from SIV and HIV-1 results in a loss of infectivity and the permeabilization of otherwise intact virions. Biochemical data, along with electron microscopy analysis, indicate that the viral membranes may contain lipid rafts and may be supported by an organized internal structure.

MATERIALS AND METHODS

Cells and reagents. The T-cell lymphoma lines, H9 and Hut78, were obtained from the American Type Culture Collection (Rockville, Md.) and maintained in complete medium (cRPMI), consisting of RPMI 1640 (Gibco-BRL/Life Technologies, Gaithersburg, Md.) containing 10% fetal calf serum (HyClone, Logan, Utah) and 10 mM HEPES (pH 7.2). LuSIV cells (50) were maintained in cRPMI with 300 μM hygromycin B (Calbiochem, San Diego, Calif.). Viruses are identified according to the virus strain and cell line in which they were propagated (virus strain/cell line; AIDS Vaccine Program [AVP], Frederick, Md.): SIV_{Mne}/HuT78 cl.E11S and HIV-1_{MN}/H9 cl.4 are both single-cell clones produced by limiting dilution (3, 45). Pharmaceutical-grade 2-hydroxy-propyl-β-cyclodextrin (Trappsol HPB, lot numbers 0100122F8 and 0902122HO) was obtained from CTD, Inc. (High Springs, Fla.).

Preparation and purification of β-CD-treated HIV-1 and SIV. Viruses were purified as described previously (5). Briefly, viruses were isolated from clarified cell culture supernatants by two successive rounds of ultracentrifugation in 25 to 50% sucrose density gradients. Virus-containing fractions were identified by UV absorption at 254 and 280 nm. Peak UV-absorbing fractions were pooled, diluted to below 20% sucrose with TNE buffer (0.01 M Tris-HCl [pH 7.2], 0.1 M NaCl, and 1 mM EDTA in deionized water), ultracentrifuged to a pellet, and resuspended in TNE buffer. Samples were stored at −80°C. For high-pressure liquid chromatography (HPLC) experiments with fresh virus, clarified cell culture supernatants were used. β-CD-treated virus was prepared by incubating virus at the indicated concentration of capsid protein in the presence of the indicated concentration of β-CD for 1 h at 37°C with gentle mixing. Virus was then repurified through a 20% sucrose pad by ultracentrifugation for 1 h at 100,000 × *g* at 4°C in either a SW28, a SW41, or a SW55Ti rotor (Beckman, Fullerton, Calif.) depending on the volume of sample to be processed. The resulting pellet obtained for each treatment condition was resuspended to the original volume. Treated, 1,000-fold-concentrated virus was divided into aliquots in small volumes and stored at −70°C.

SDS-PAGE and Western blotting. For silver staining and Western blotting (immunoblotting), equal volumes of an aliquot of the viral samples were loaded onto separate sodium dodecyl sulfate-polyacrylamide gel electrophoresis (SDS-PAGE) 4 to 20% gradient gels (Novex, San Diego, Calif.) under reducing conditions. One gel was developed with the SilverXpress silver staining kit (Invitrogen, Carlsbad, Calif.). A matched gel was used for immunoblotting. Proteins were transferred onto an Immobilon-P membrane (Millipore, Bedford, Mass.) and briefly developed with Ponceau S to mark unstained molecular weight markers (Novex). Rabbit polyclonal antisera was used to detect the following SIV proteins: gp120 (DJ-36603; AVP) and reverse transcriptase and integrase (RT [no. 366A] and IN [no. 373], respectively; both generous gifts from J. Levin). Monoclonal antibodies were used to detect HIV-1 gp120 (BF5-D5-F8) and SIV p28 (94-01P1F5), and HIV-1 p24 and (96-0020) (all from AVP). Goat anti-mouse or goat anti-rabbit horseradish peroxidase-conjugated secondary antibodies (Jackson Laboratories, Bar Harbor, Maine) were revealed by using enhanced chemiluminescence (Amersham Life Sciences, Arlington Heights, Ill.). Densitometry was performed from scanned images of immunoblot films with Scan Ace III (Pacific Image Electronics) in the TIFF file format. Band intensities were quantified by using Scion image analysis software (Scion Corp., Frederick, Md.). The relative intensity ratios of the bands being analyzed were not altered. Appropriate exposures were used to ensure that the measured intensities were within the range of the optical hardware.

Cholesterol measurement. Cholesterol was measured with an Amplex Red cholesterol kit (Molecular Probes, Eugene, Oreg.).

HPLC. Viral samples were disrupted in 8 M guanidine-HCl (Pierce, Rockford, Ill.) with or without 50 mM dithiothreitol (Calbiochem) and then fractionated by HPLC to isolate viral proteins. HPLC was performed at a flow rate of 300 μl/min on a Poros R2/H narrow-bore column (2.1 by 100 mm; Boehringer, Mannheim, Germany) by using aqueous acetonitrile-trifluoroacetic acid solvents and a Shimadzu HPLC system equipped with LC-10AD pumps, an SCL-10A system controller, a CTO-10AC oven, an FRC-10A fraction collector, and an SPD-M10AV diode array detector. The gradient of buffer B (0.1% trifluoroacetic acid in acetonitrile) was as follows: 10 to 36.5% for 12 min, 36.5 to 37% for 4 min, 37 to 41% for 7 min, 41 to 70% for 12 min, and 70% for 5 min. A temperature of 55°C was maintained during HPLC separation. Peaks were detected by UV absorption at 206 and 280 nm and analyzed by sequencing by using an automated Applied Biosystems 477 protein sequencer, by SDS-PAGE, and by immunoblot analysis with an enhanced chemiluminescence procedure (Amersham Life Sciences). Quantitation of total viral and purified proteins was performed by amino acid analysis with a Hitachi L-8800 amino acid analyzer.

Quantitation of viral RNA. Particle-associated SIV Gag RNA was quantitated as previously described on a Prism 7700 sequence detection system (PE Biosystems, Foster City, Calif.) (30). Specimen preparation were as previously described (55), with modifications (J. D. Lifson, unpublished data). Particle-associated HIV-1 Gag RNA assays were carried out by using the Roche Amplicor monitor system (detection limit, 400 copies/ml; Roche Diagnostic Systems, Nutley, N.J.).

Virus titer determinations. Virus replication and titers were determined by infection of LuSIV cells as previously described (50). Briefly, 2×10^5 LuSIV cells were inoculated with 10-fold serial dilutions of the indicated treated virus in triplicate into a 96-deep-well plate (2.2 ml; Marsh Biomedical Products, Inc., Rochester, N.Y.), followed by incubation at 37°C. Cells were cultured in RPMI 1640 with 10% heat-inactivated lipoprotein-depleted fetal bovine serum (Sigma, St. Louis, Mo.). Cells were harvested 60 h after infection, and luciferase expression was analyzed with a commercial luciferase assay system (Promega, Madison, Wis.). Wells exhibiting luciferase activity greater that the mean of the negative controls plus three standard deviations were scored as positive, and the 50% tissue culture infective dose(s) ($TCID_{50}$) was calculated by the method of Reed and Muench (48).

Electron microscopy. Electron microscopy was done by M. Gignac and K. Nagashima (Laboratory of Cell and Molecular Structure, SAIC-Frederick, NCI-FCRDC, Frederick, Md.). The treated or untreated virus was fixed with 1.25% (vol/vol) glutaraldehyde in phosphate-buffered saline. Cell pellets were embedded and processed as previously described (16). Embedded virus pellets were sectioned and examined in a Hitachi H-7000 electron microscope operated at 75 kV. Virus particle images were captured with a digital camera at 1,024 × 1,024-pixel resolution and stored as TIFF files. Images were processed with Adobe Photoshop (Adobe Systems, Inc., Mountain View, Calif.).

RESULTS

β-CD treatment of either SIV or HIV-1 results in permeabilization of virions. To test the hypothesis that cholesterol removal from cell-free virion particles may be disruptive, purified SIV and HIV-1, fixed at concentrations of 2 and 3.5 μg/ml of capsid protein equivalents, respectively, were treated with increasing concentrations of β-CD for 1 h at 37°C and repurified through 20% sucrose by ultracentrifugation. Silver staining and Western blotting of the samples was done to determine whether virion-associated proteins were lost (Fig. 1). Permeabilization was defined as a greater decrease in the signal intensity for the capsid protein relative to the signal for the envelope glycoprotein (gp120). A slight loss of signal for the internal capsid protein (p28) relative to signal for gp120 occurred at 20 mM β-CD in SIV, and p28 was clearly lost at 80 mM β-CD (Fig. 1A, C, and E). The amount of SIV membrane-associated gp120 showed only a modest reduction through the concentration range up to 80 mM but was clearly diminished at a β-CD concentration of 160 mM (Fig. 1C and E). In HIV-1 the ratio of p24 to gp120 was fairly constant up to a β-CD concentration of 80 mM, when p24 was lost (Fig. 1B, D, and F). The HIV-1 gp120 signal was relatively unchanged throughout the treatment range (0 to 160 mM β-CD) (Fig. 1D and F). The decrease in signal intensity for gp120 in the untreated (none) versus 0 mM treatment (virus incubated in buffer for 1 h and

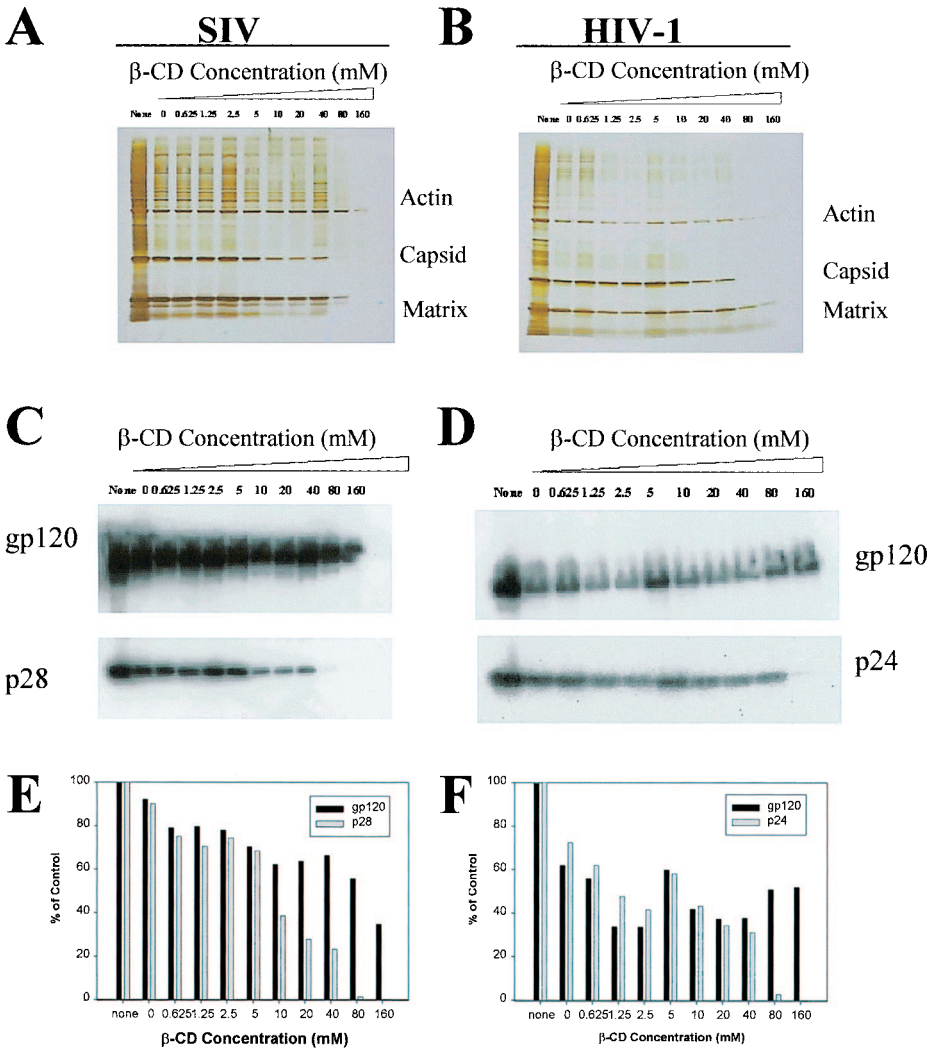

FIG. 1. Treatment of fixed concentrations of SIV and HIV-1 with increasing concentrations of β-CD results in permeabilization of the viral membrane and loss of capsid protein. A fixed amount of either SIV (A, C, and E) or HIV-1 (B, D, and F) was treated with increasing concentrations of β-CD for 1 h at 37°C. Samples were analyzed by SDS-PAGE and silver staining (A and B). Levels of gp120 and capsid (p28 for SIV; p24 for HIV) were determined by Western blotting (C and D), and band intensity was determined by densitometry analysis (E and F). Bars: ▨, densitometry results for gp120; ■, densitometry results for capsid protein. None, concentrated virus stock prior to processing.

repurified through sucrose) represents virus that is lost during the repurification procedure (Fig. 1). To ensure that the observed effect was not merely due to high concentrations of β-CD but also represented a reproducible effect that correlated with the ratio of cholesterol to β-CD, we performed an experiment similar to the one above, except the β-CD concentration was fixed at 20 mM and the virus concentration was varied (Fig. 2). SIV permeabilization, as indicated by the higher loss of capsid protein relative to the envelope protein, was evident by densitometry measurement of bands at 4 μg/ml of p28, but the SIV was clearly depleted of capsid protein at 2 μg/ml of p28 (Fig. 2A, C, and E). gp120 levels for SIV remained stable over the concentration of virus tested. HIV-1 permeabilization, as indicated by the greater loss of core proteins relative to envelope protein, occurred at 4 μg/ml of p24 (Fig. 2B, D, and F). Fluctuations of signal for gp120 of up to 20% (Fig. 1 and 2) were probably attributable to variability in recovery of the viral pellet after repurification of virus through sucrose.

Permeabilization of virions correlates with a complete removal of cholesterol from virions, and cholesterol depletion follows a biphasic pattern. To determine the relationship between viral membrane permeabilization and residual amounts of cholesterol in the virion, virus samples were assayed to measure the residual cholesterol content in viral preparations after exposure to a range of β-CD concentrations (Fig. 3). When the concentration of β-CD was varied, the measurements of residual cholesterol indicated that a plateau was reached for HIV-1 at between 1.25 and 5 mM β-CD and a sharp drop occurred at >10 mM β-CD (Fig. 3A). Similarly, SIV treatment resulted in a plateau of residual cholesterol at concentrations between 0.625 and 5 mM β-CD (Fig. 3A), followed by a second phase of more gradual decline of cholesterol at higher concentrations. The observed plateau suggests that

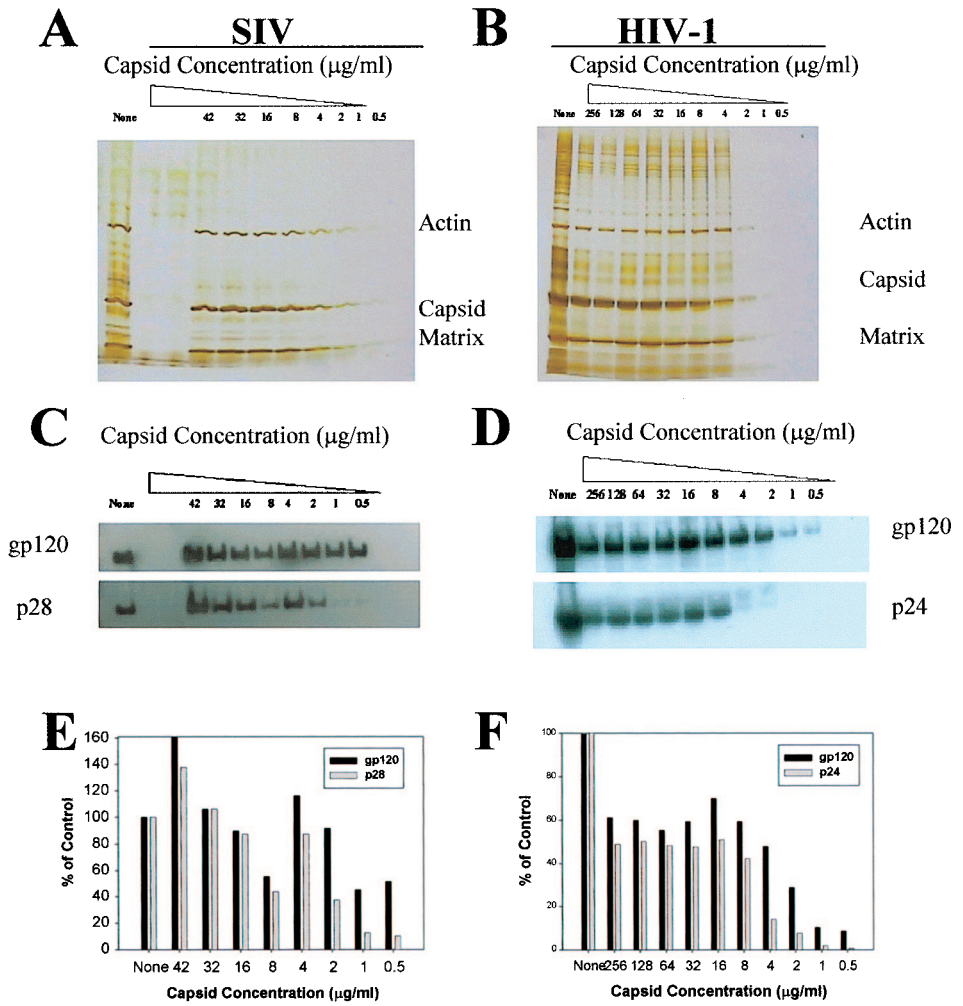

FIG. 2. Treatment of either SIV or HIV-1 with fixed concentrations of β-CD and decreasing concentrations of virus resulted in permeabilization of the viral membrane and loss of capsid protein. Decreasing concentrations of capsid for either SIV (A, C, and E) or HIV-1 (B, D, and F) were treated with 20 mM β-CD for 1 h at 37°C. Samples were analyzed by SDS-PAGE and silver staining (A and B). Levels of gp120 and capsid (p28 for SIV and p24 for HIV) were determined by immunoblotting (C and D), and the band intensity was determined by densitometry analysis (E and F). Bars: ▨, densitometry results for gp120; ■, the densitometry results for capsid protein. None, concentrated virus stock prior to processing.

cholesterol removal from SIV and HIV-1 followed a biphasic pattern, suggesting that virions may have distinct pools of virion-associated cholesterol as previously described (17), a finding consistent with the presence of virion-associated lipid rafts. Permeabilization, as indicated by a loss of capsid for both HIV-1 and SIV, correlated with the removal of cholesterol to levels below the limits of detection of the assay used (Fig. 3A). The difference in the amounts of cholesterol measured in the two viruses may reflect the difference in starting virus concentrations of 2 and 3.5 μg/ml of capsid protein for SIV and HIV-1, respectively; however, the cholesterol content varied from virus preparation to preparation and did not correlate strongly with capsid concentration, suggesting that the cholesterol content of virions is dependent on the cell line used and the conditions of cell growth at the time of virus harvest. Therefore, to determine whether the molar ratios of β-CD to virion-associated cholesterol determined whether permeabilization occurred, the initial amount of cholesterol in each virus sample was measured and the molar ratios of β-CD to virion-associated cholesterol were calculated by dividing the moles of β-CD used under each condition by the moles of cholesterol present in each virus sample. Figure 3B shows the molar ratios of β-CD: cholesterol under each treatment condition.

Permeabilization of both SIV and HIV-1 occurred at a molar ratio of β-CD to cholesterol of >80. Since the cholesterol content of virus preparations varies, we were able, by utilizing this method of calculating ratios, to predict when permeabilization would occur, and we have now reproducibly prepared multiple preparations of permeabilized and nonpermeabilized HIV-1 and SIV.

Permeabilization results in the loss of several core proteins. To extend our understanding of the effect of β-CD to other viral and host proteins present in the virus preparation, virions were prepared under permeabilizing (β-CD/cholesterol ratios of >300) and nonpermeabilizing conditions (β-CD/cholesterol ratios of <60) for HPLC analysis as previously described (10). Virus input was normalized to gp120 content, as determined by SDS-PAGE, immunoblotting, and densitometry. Under non-

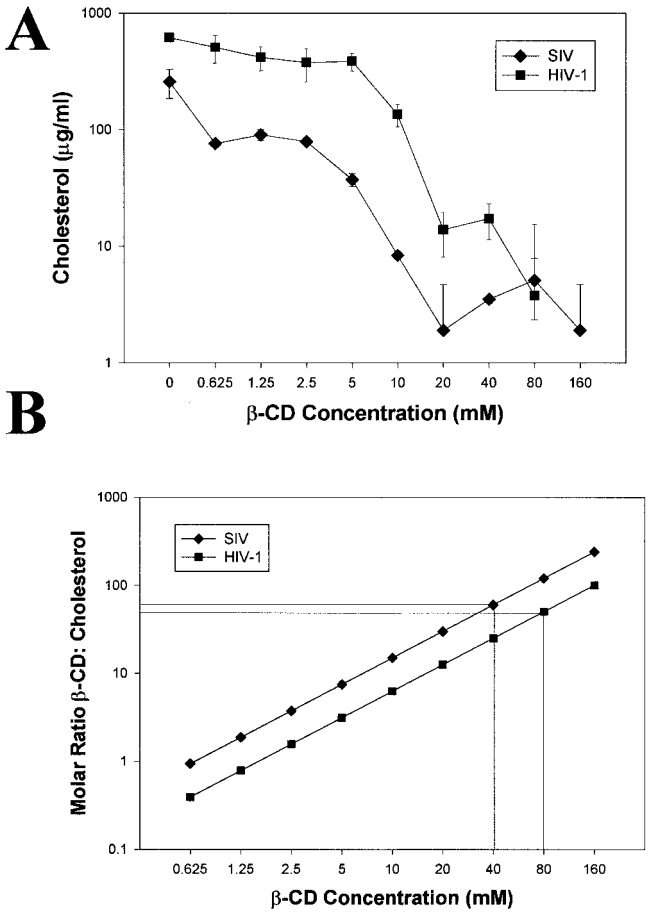

FIG. 3. Permeabilization correlated with total depletion of cholesterol from virus and could be predicted based on the ratio of β-CD to cholesterol present in the sample. Residual cholesterol was measured in both SIV and HIV-1 treated with increasing concentrations of β-CD (A). The ratio of β-CD to the initial cholesterol level was calculated for SIV and HIV for each set of treatment conditions (B), and permeabilization levels estimated from Fig. 1 are indicated by intersecting solid lines. Error bars represent the standard deviation of the mean.

permeabilizing conditions, both SIV and HIV-1 virions showed a reduction in the cholesterol peak (Fig. 4A and B). The slight reduction in the signal for p8 in SIV under nonpermeabilizing conditions (Fig. 4A) was recovered under reducing conditions (data not shown). HIV-1 also appeared to have slight reduction in the signal for p6 after treatment under nonpermeabilizing conditions. SIV that was prepared under permeabilizing conditions showed a marked loss of the internal viral proteins p8, p1, p6, matrix, and capsid (Fig. 4C). Viral envelope proteins gp120 and gp41 were unaffected, as were the host proteins HLA class I and class II, which are incorporated into the viral membrane. Host proteins that are incorporated inside of the virion (actin, moesin, and ezrin) were also unaffected. HIV-1 prepared under permeabilizing conditions also demonstrated a marked loss of p1, p6, and capsid and, to a lesser extent, NC and matrix proteins (Fig. 4D). As with SIV, host proteins incorporated into the membrane of the virus were not affected, nor were the levels of actin. Particle-associated gp120 levels were also not affected by β-CD treatment of HIV-1, as determined by immunoblotting (data not shown). The retention of NC protein in HIV-1 increased if the virus was oxidized (data not shown) (2). Similar results were obtained when freshly isolated virus was used in place of frozen viral stocks (data not shown).

Differential retention of RT and IN in permeabilized SIV and HIV-1. Since RT and IN are critical enzymes required to establish infection and are obscured in HPLC analysis by host proteins, Western blotting was used to detect these proteins in permeabilized virus preparations. SIV and HIV-1 (same stocks as in Fig. 1) were normalized for input gp120 (by Western blotting) and probed for RT and IN (Fig. 5). The signal for RT and IN was significantly reduced at the 40 mM concentration of β-CD in SIV and was below the limit of detection at the 80 and 160 mM levels of β-CD (Fig. 5A). In contrast, although there was a significant reduction in the signal for RT in HIV-1 at the 80 mM level of β-CD and above, the weak signal was retained even at 160 mM β-CD (Fig. 5B). Integrase was retained in HIV-1 throughout the concentration range of β-CD in contrast to SIV (Fig. 5B).

SIV and HIV-1 lose viral RNA upon permeabilization. To determine whether viral RNA was retained in SIV and HIV-1 after permeabilization by β-CD, virions from Fig. 1 were subjected to RNA analysis by RT-PCR with probes for Gag. Virion associated SIV and HIV-1 Gag RNA was measured as described in Materials and Methods. The results obtained showed a 89 and 98% reduction in the amount of viral RNA in SIV at 80 and 160 mM β-CD, respectively, showing that SIV particles lost viral RNA after permeabilization with β-CD (Fig. 6A). Viral RNA was also significantly reduced in HIV-1 upon permeabilization but less than in SIV (68 and 87% of viral RNA at 80 and 160 mM β-CD, respectively) (Fig. 6B).

Treatment of HIV-1 or SIV with β-CD results in a dose-dependent inactivation of virus. To determine what effect cholesterol depletion and permeabilization had on both infectivity and viral replication, samples of virus from the same preparations used in the above experiments were assayed for infectivity on an SIV luciferase tat transcomplementation reporter cell line (LuSIV) as previously described (50). When LuSIV cells were infected with virus treated with various concentrations of β-CD and assayed for luciferase expression 60 h after virus exposure, we found a dramatic decrease in the replication (indicated by mean luciferase expression) of both SIV and HIV-1 at concentrations of β-CD of ≥10 mM (Fig. 7A and B). The dynamic range of the luciferase assay is such that weakly positive signals (>2 standard deviations above the negative control) do not show up as positive in graphs displaying the data. However, $TCID_{50}$ calculations take into account the wells that are weakly positive, making the $TCID_{50}$ approach a much more sensitive method of determining residual infectivity after β-CD treatment. We thus calculated the $TCID_{50}$ values for viruses that had been treated with β-CD and added to the reporter cells. The $TCID_{50}$ results show that β-CD treatment reduces HIV and SIV infectivity by as much as 4 and 5 logs, respectively (Fig. 7C and D). The results showed that infectivity is abolished in a dose-dependent manner and is reduced to levels below the limit of detection once the virions are permeabilized.

Permeabilized SIV or HIV-1 virions have holes in their membranes. To determine the morphology of particles recovered after β-CD treatment, SIV and HIV-1 were prepared

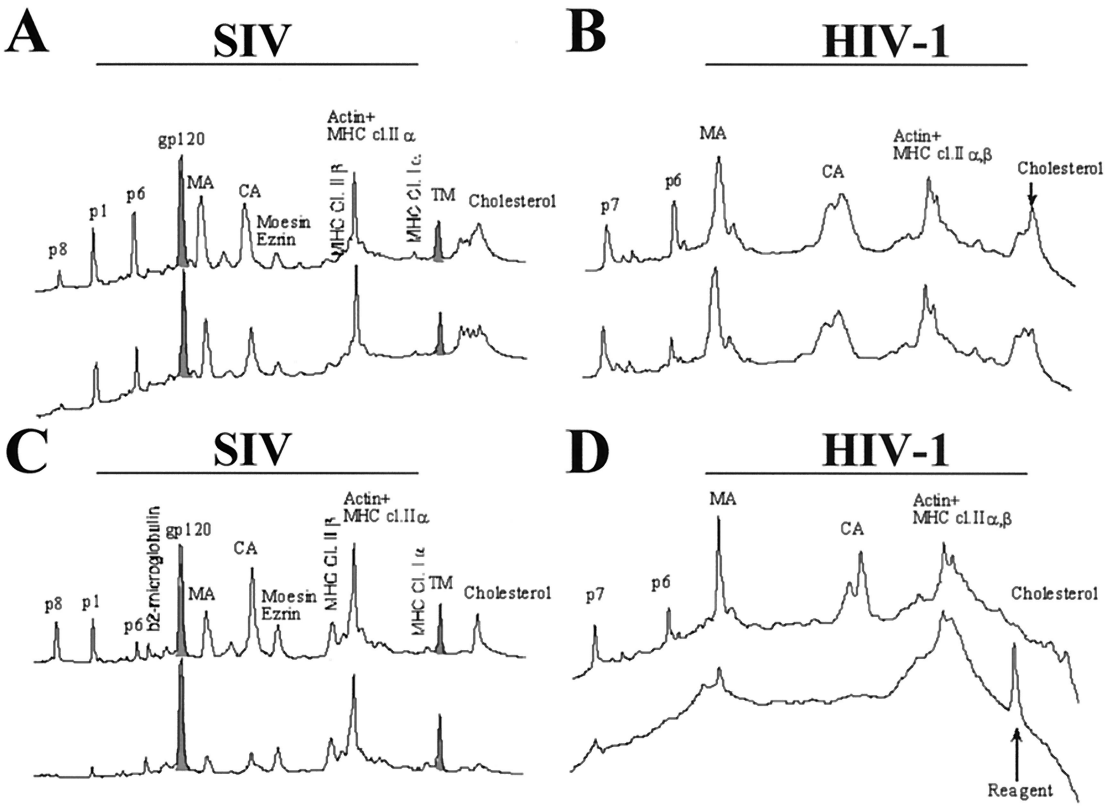

FIG. 4. Treatment of SIV or HIV-1 under nonpermeabilizing conditions resulted in loss of cholesterol, whereas treatment of SIV or HIV-1 under permeabilizing conditions resulted in loss of proteins found inside the virion. Concentrated SIV was diluted and prepared under nonpermeabilizing (A) or permeabilizing (C) conditions and was examined by HPLC. Concentrated HIV-1 was diluted and prepared under nonpermeabilizing (B) or permeabilizing (D) conditions and examined by HPLC. The upper trace is untreated virus, and the lower trace is β-CD-treated virus in all four panels. Loading was corrected for gp120 content. Peaks were identified by amino acid analysis and are indicated on the upper trace.

under permeabilizing and nonpermeabilizing conditions as described above and then examined by transmission electron microscopy. SIV prepared under nonpermeabilizing conditions (Fig. 8B and E) was very similar in morphology to control virus (Fig. 8A and D). In contrast, SIV prepared under permeabilizing conditions had a markedly different morphology from that of control virus (Fig. 8C and F to I). The most striking difference was that large gaps in the membrane were evident in the permeabilized virus (see arrows in Fig. 8C and F to I). Permeabilized virions appeared to have single large holes in their membranes (Fig. 8H and I). HIV-1 prepared under nonpermeabilizing conditions (Fig. 9B and E) was very similar in morphology to control virus (Fig. 9A and D). In contrast, HIV-1 prepared under permeabilizing conditions (Fig. 9C and F to K), similar to SIV, had a markedly different structure from that of the control virus. Again, large single gaps in the particle membrane were evident in the permeabilized virus (see arrows in Fig. 9C and F to K), although, rarely, a particle appeared to have two holes (Fig. 9I). In both viruses, permeabilized virions also appeared to have a less electron-dense core than control virus and the core appeared to be generally proximal to the hole in the viral membrane (acentric). The membrane of the permeabilized virions also appeared to be of irregular thickness, compared to control virus, especially in proximity to the holes. It is important to note that although large holes were clearly visible in the membrane of virus prepared under per-

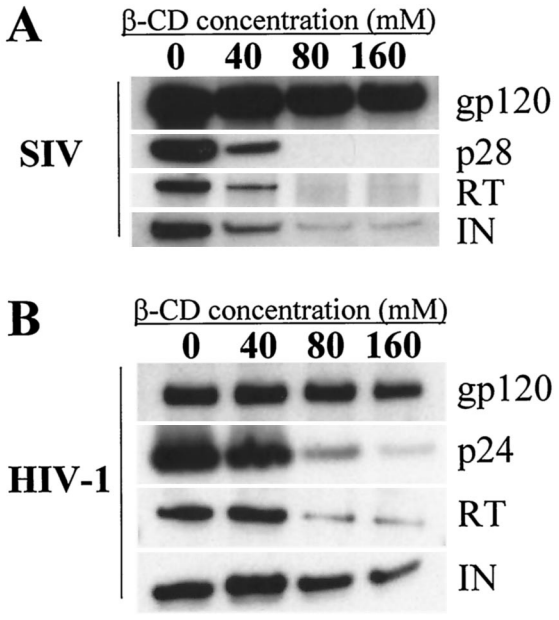

FIG. 5. Differential retention of RT and IN in permeabilized SIV and HIV-1. Stocks of virus prepared for Fig. 1 were normalized to gp120 content and RT, IN, and capsid protein were examined by immunoblotting. (A) Results obtained for SIV; (B) results obtained for HIV-1.

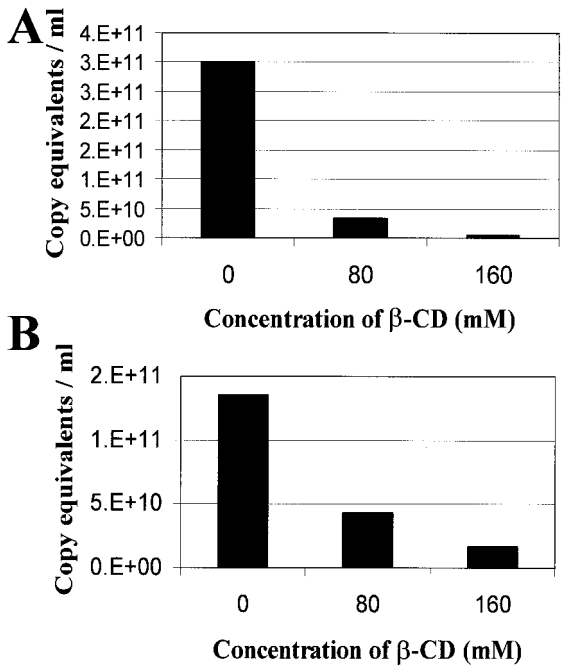

FIG. 6. SIV and HIV-1 lose viral RNA upon permeabilization. Stocks of virus prepared for Fig. 1 were analyzed for particle-associated viral RNA by real-time RT-PCR. (A) Results obtained for SIV; (B) results obtained for HIV-1. Virus input was normalized to gp120 content.

meabilizing conditions, the virions, which were not fixed before β-CD treatment, were otherwise intact. This suggests that the viral membrane is not solely responsible for maintaining virion size, shape, and integrity as discussed below. The "cores," as seen in permeabilized viruses in Fig. 9, are often irregularly shaped and positioned. Based on the real-time PCR data shown above, these structures may not contain RNA. Definitive identification of the core composition in permeabilized virus will require further study.

DISCUSSION

In the present study we examined the effect of cholesterol depletion by β-CD on the structure and infectivity of HIV-1 and SIV. In agreement with other studies, HIV-1 infectivity was decreased in a dose-dependent manner (20) and SIV was affected in a similar manner, when the viruses were treated with β-CD. We also found that HIV-1 and SIV viral membranes were permeabilized when treated with ratios of β-CD to cholesterol of >80. Permeabilization correlated with the removal of cholesterol from the virus to very low levels and caused the loss of internal viral proteins. Permeabilization of virions by nonionic detergents has also been reported to occur within a narrow window of detergent concentrations (60). Electron micrographs of HIV-2 prepared by fixation and treatment with 1% NP-40 show a morphology similar to that of the virions reported here, with acentric cores and holes in the membrane (46). Virion permeabilization with β-CD was distinct from these previous studies, since permeabilization resulted in holes large enough passage of fairly large proteins in addition to small ions or metabolites (38, 61). The results of the current study were somewhat surprising since the virions were not fixed prior to β-CD treatment and yet showed large holes, clearly indicating that membrane integrity had been compromised. Presumably, the edge of the holes were stabilized by "hairpinning" of the lipid bilayer, resulting in a lipidic pore. We cannot exclude the possibility that some impurity in the β-CD is responsible for the permeabilization effect; however, multiple lots were tested to ensure reproducibility (data not shown), and the β-CD was pharmaceutical grade. Permeabilization correlated very well with cholesterol depletion and virus could be permeabilized by fixing the β-CD concentration at 20 mM and varying the virus input. Thus, it is unlikely that permeabilization is attributable to an impurity in the β-CD. It is possible that at the high concentrations of β-CD at which the holes are formed other lipids, in addition to cholesterol, may be lost, critically destabilizing the viral membrane in local areas.

Measuring the residual cholesterol in SIV and HIV-1 exposed to increasing concentrations of β-CD showed that there are two pools of cholesterol in the virions. The bimodal pattern of cholesterol depletion of virions is in agreement with that observed previously in cells and HIV-1 (17, 21, 25, 59). The two pools likely represent cholesterol that is either tightly associated with sphingolipids and proteins (slow pool/lipid raft-associated) or is not tightly associated with other molecules (fast pool/non-raft associated) and is therefore difficult or easy to remove, respectively (21, 59). This observation suggests that the membranes of HIV-1 or SIV particles are organized into lipid raft and nonraft regions similar to the plasma membranes of host cells, an idea in agreement with findings from Gordon et al., who used electron spin resonance spectroscopy (ESR) to demonstrate cholesterol-rich and cholesterol-poor regions in the membrane of HIV-1 (17).

In the present study the infectivity of HIV-1 and SIV was reduced in dose-dependent fashion at β-CD concentrations greater than 10 and 5 mM, respectively, and the loss of infectivity was closely associated with reduction in virion cholesterol. Reduction of infectious titers to below threshold levels of detection correlated with virus permeabilization, suggesting that virion infectivity is not completely lost until lipid-raft associated (slow pool) cholesterol is removed from the viruses. The loss of viral infectivity after cholesterol depletion is likely due to a combination of factors: inihibition of fusion, loss of virion-associated cholesterol, loss of mature Gag and Pol proteins, loss of viral RNA, and destruction of some virions. We have shown that infectivity of HIV treated with nonpermeabilizing concentrations of β-CD can be restored by replenishing viral cholesterol (unpublished results). However, we were unable to restore virus infectivity by adding back cholesterol to permeabilized virions (data not shown). Presumably, the large holes in the viral membrane cannot be repaired by cholesterol alone, and patching the membrane probably cannot overcome loss of critical viral proteins and RNA.

Wilk et al. showed that viral RNA is maintained in subviral particles upon detergent lysis, whereas matrix and capsid molecules are released (58). In our studies, internal viral proteins were lost in both SIV and HIV-1, with the notable retention of some NC, MA, and RT and virtually complete retention of integrase in HIV-1. The viral RNA, reduced very significantly, also appeared to be more efficiently retained in HIV-1. Since

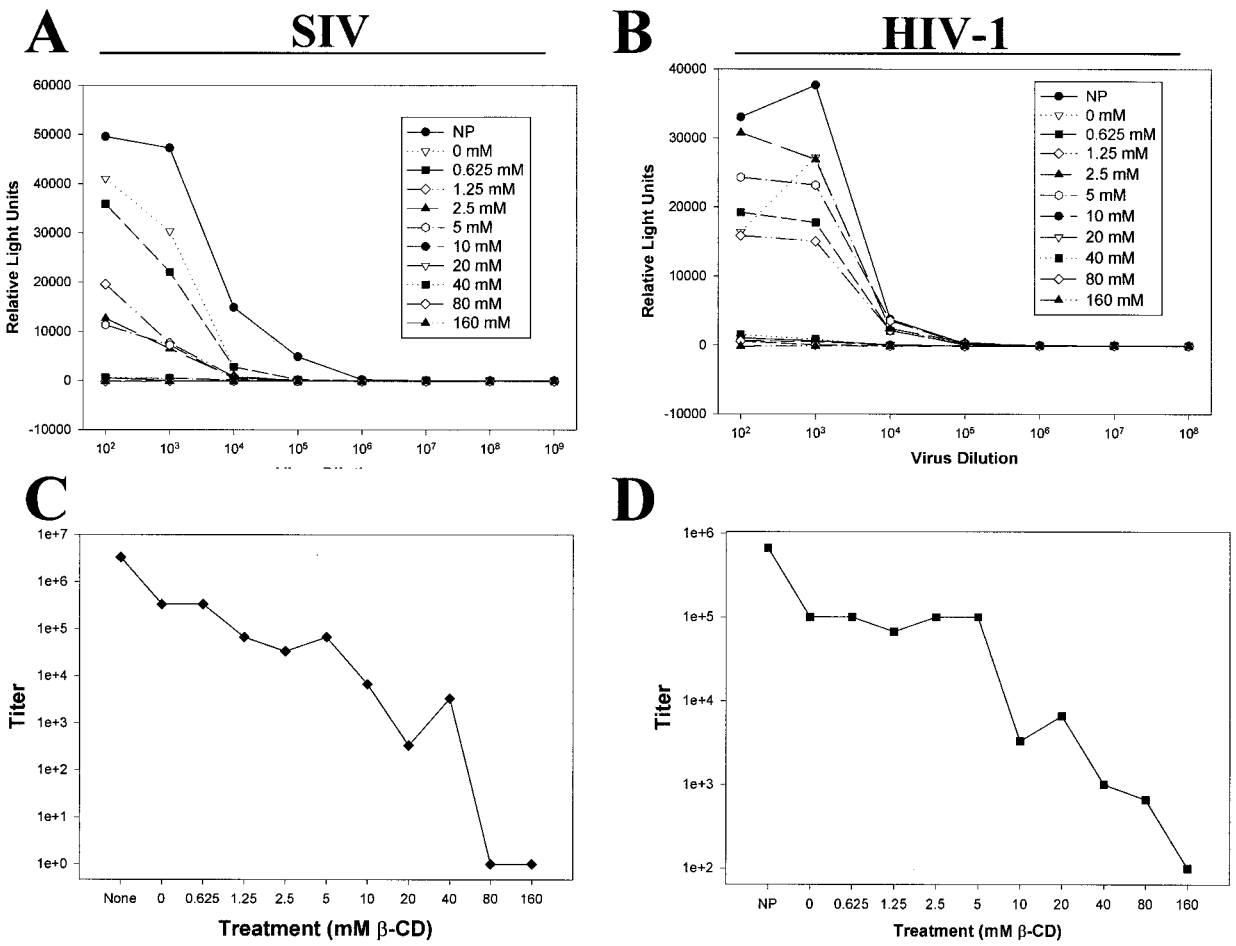

FIG. 7. Suppression of viral replication and loss of titer correlate with treatment of either SIV or HIV-1 with increasing doses of β-CD. Stocks of virus prepared for Fig. 1 were analyzed for both replication and infectivity on a cell line (LuSIV) that expresses luciferase upon infection with either SIV or HIV-1. SIV (A and C) or HIV-1 (B and D) was treated with increasing concentrations of β-CD (see legend in figure). Viral replication as measured by luciferase expression was then determined (A and B), and titers were calculated (C and D), under limiting dilution. Luciferase levels were measured 60 h after infection of the indicator lines. The mean luciferase value of three replicate wells is given for each dilution (A and B). The titer is expressed as the reciprocal dilution of the lowest dilution at which a positive well was scored (C and D). NP, concentrated viral stock not processed.

all of the retained proteins in HIV-1 are thought to be associated with the ribonucleoprotein complex (19), the partial retention of viral RNA in permeabilized HIV-1 may be responsible for retention of these proteins. The loss of RNA from permeabilized viruses raises the question of what is the nature of core-like structures in these particles revealed by electron microscopy. Since host cytoskeletal proteins are retained in permeabilized viruses, these proteins could contribute to the residual electron density. Retroviruses may be quite heterogeneous, and it is therefore possible that permeabilized virions with core-like structures represent a subpopulation of treated particles that retain RNA. To minimize heterogeneity, we used molecular clones, and most permeabilized virions appeared to have irregular core-like structures. It is not clear whether the presence of permeabilized virions with core-like structures correlates with the amount of residual viral RNA retained after virus permeabilization. Immunoelectron microscopy and careful particle counting will have to be done before we can address this question.

The striking morphology of SIV and HIV-1 particles that were permeabilized by β-CD treatment in the present study is reminiscent of p6 mutant virions that are defective in budding and attached to cells by a thin membranous tether (15, 18). Further, the holes in β-CD-permeabilized virions appear to be approximately the same size as the region of the virus membrane tethered to the host cell in the aforementioned budding mutants, as well as the region of the virus membrane that overlies the gap in the submembrane Gag polyprotein precursor complex in immature virions (14, 15, 18). These previous observations, combined with those of the present study, raise the intriguing possibility that HIV-1 and SIV virions carry "scission plaques." These scission plaques may represent stable specialized lipid rafts on the virus membrane that are involved in virus fission and possibly fusion. A specialized viral membrane region that organizes the viral budding machinery has been suggested previously. Craven et al. (11) suggested that Rous sarcoma virus contains an organized microdomain, revealed as a prominent bleb in the envelope of Rous sarcoma virus when the major homology region of capsid is mutated. Consistent with the presence of a scission plaque on HIV-1 and

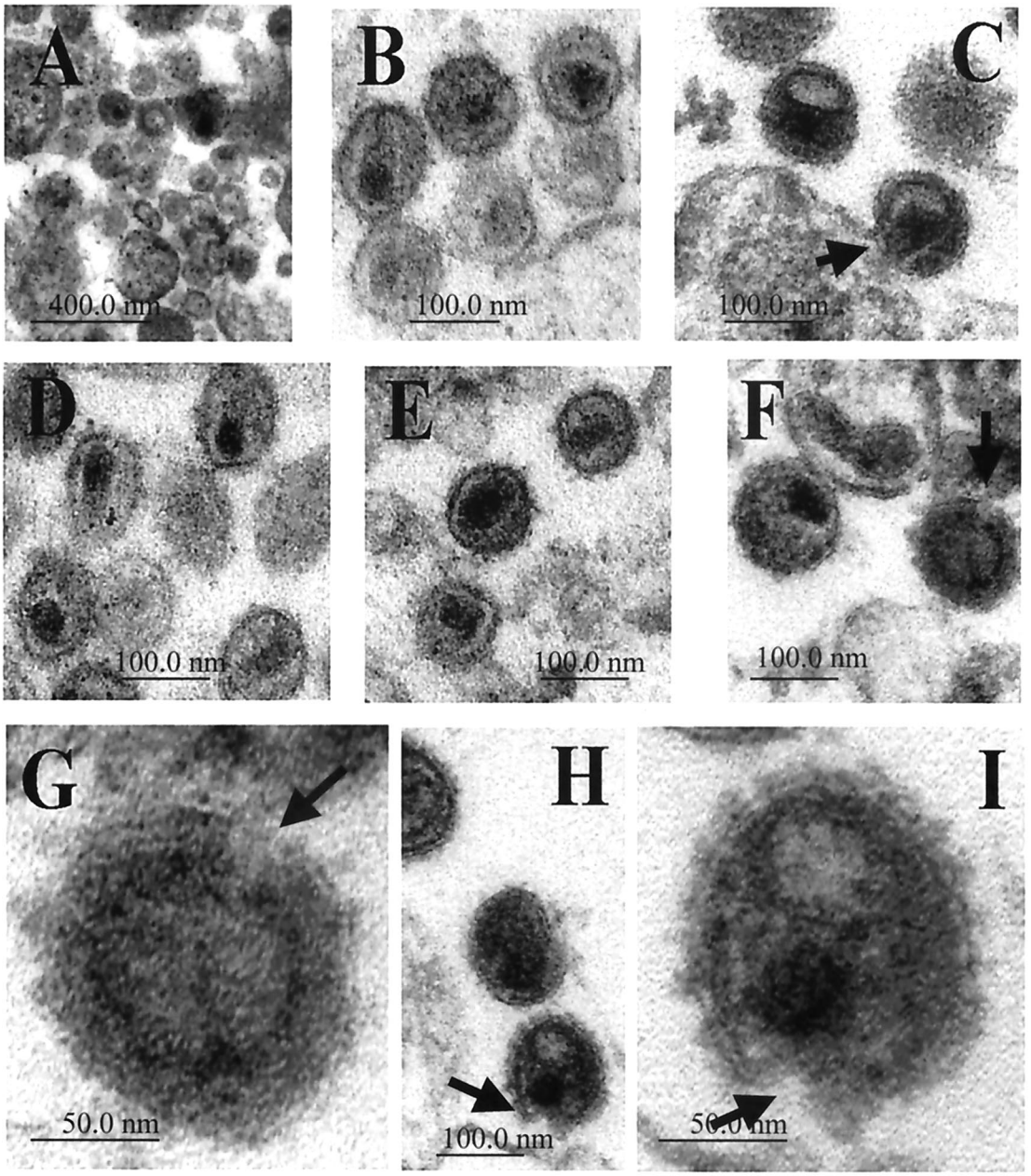

FIG. 8. Electron microscopy of SIV treated under permeabilizing conditions revealed holes in the membrane of the virus. SIV samples that were untreated (A and D), treated under nonpermeabilizing conditions (B and E), or treated under permeabilizing conditions (C and F to I) were examined by transmission electron microscopy. Panels G and I are larger magnifications of the images in panels F and H, respectively. Magnifications: ×4,000 (A), ×20,000 (B to F and H), and ×40,000 (G and I).

SIV, we generally observed a single large gap in both viral membranes. However, due to the nature of transmission electron microscopy, it is impossible to know for certain if more than one hole is present. Three-dimensional reconstruction of transmission electron microscopy images or other ultrastructural approaches will be necessary to clarify this important issue. Other evidence for lipid rafts on HIV-1 virion particles comes from electron microscopy studies showing localization of GPI-anchored proteins CD55 (DAF) and CD59 (HRF-20) to one pole of the virions (36). A caveat is that the processing of virions in these earlier studies may have induced capping or clustering of the molecules as can occur in cells.

The results reported here add to the growing evidence for the existence of an organized protein scaffold or "viroskeleton" inside of HIV-1 and SIV, associated with the membrane, that may be responsible for maintaining virion integrity. This proposed protein scaffold is distinct from the RNA scaffold upon which the core is constructed. The host cell cytoskeleton has been implicated in many aspects of the HIV-1 virus life cycle, including viral assembly (32, 35, 49), budding (49, 52), entry

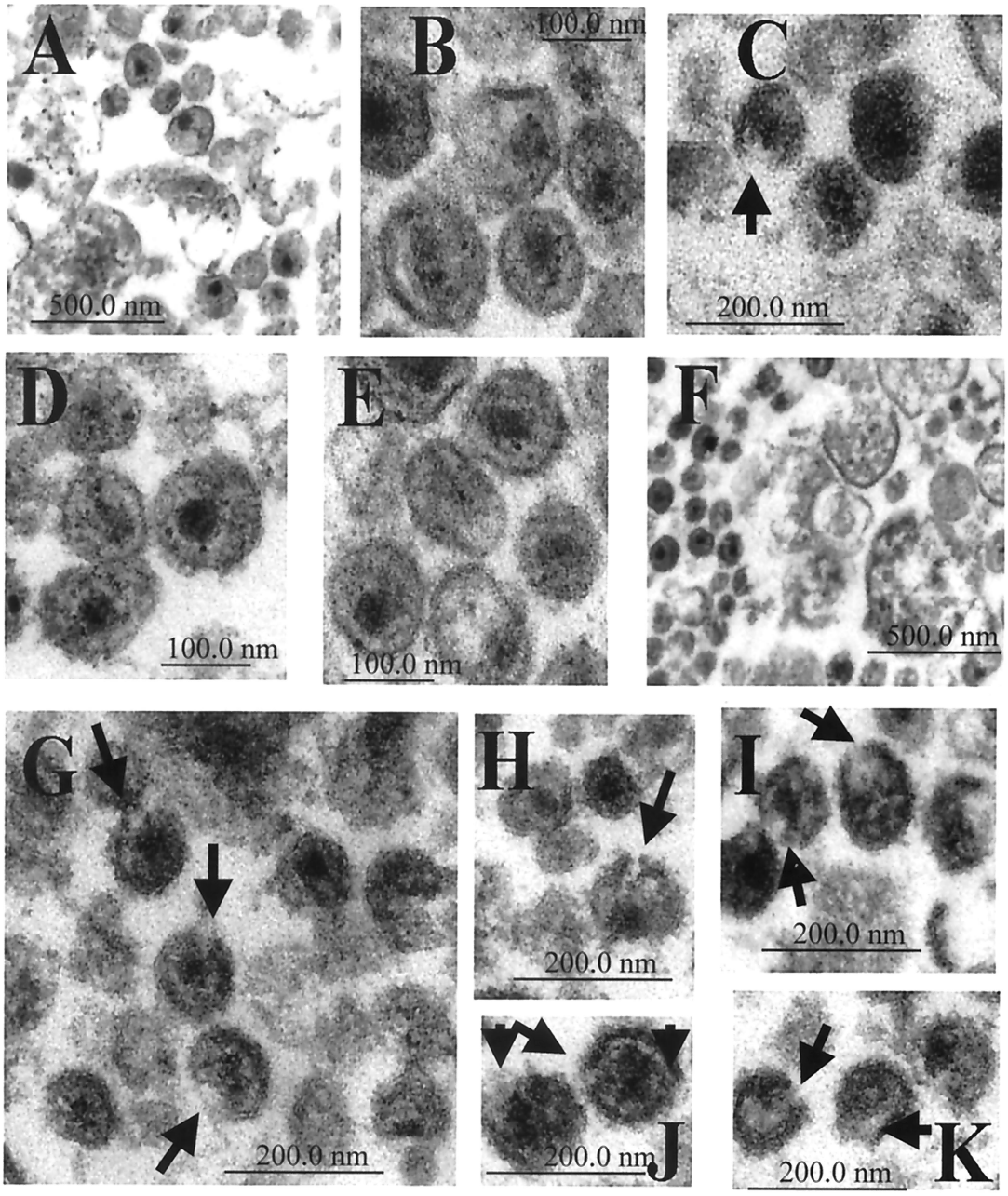

FIG. 9. Electron microscopy of HIV-1 treated under permeabilizing conditions revealed holes in the membrane of the virus. HIV-1 samples that were untreated (A and D), treated under nonpermeabilizing conditions (B and E), or treated under permeabilizing conditions (C and F to K) were examined by transmission electron microscopy. Magnifications: ×4,000 (A and F) and ×20,000 (B to E and G to K).

(23), and early steps in reverse transcription (8). Additionally, cytoskeletal components are required during transport of the preintegration complex to the nucleus (19). Several host molecules, including host cytoskeletal and cytoskeletal binding proteins, are incorporated into HIV-1 and SIV upon release from the cell (42–44). Actin is a substrate for viral protease activity (35, 53, 54, 56, 58) but when complexed with NC it is protected from cleavage (58). Actin or other cellular cytoskeletal components may participate in viral assembly and viral maturation and ultimately form part of the viroskeleton that maintains virion integrity. Since most HIV-1 and SIV preparations are contaminated with microvesicles (4), which contain actin, the presence of actin in virions may be overestimated. However, the amount of actin, moesin, and ezrin attributed to the virion itself comprises ca. 10 to 15% of the total amounts of these proteins in virus preparations (43), so it is clearly possible that they could contribute to the formation of an intravirion protein complex. The possibility that these molecules may be organized and contiguous with the membrane of the virion is further indicated by recent reports that there are interactions between the cytoplasmic tail of gp41 and cytoskeleton proteins and cytoskeletal regulatory proteins (26, 62).

This is a particularly interesting observation given the difference in protein and viral RNA retention between SIV and HIV-1 reported here, since the gp41 of SIV used in the present study has a truncated cytoplasmic tail, whereas the cytoplasimic tail of the HIV-1 gp41 is full length. We have demonstrated that integrins incorporated by HIV-1 (41) are constitutively active (unpublished results), and this observation also supports the presence of an organized protein complex associated with the viral membrane. Given the involvement of lipid rafts and cytoskeleton components in regulating integrin function in cells (28, 34), integrins may be perpetually activated on HIV-1 because of their presence in virion lipid rafts and association with complexes containing host cytoskeletal components inside of the virions.

The observation that β-CD-treated virus is inactivated and permeabilized provides valuable insights for the development of β-CD as a topical microbicide for AIDS prophylaxis. β-CD has already been shown to be efficacious in a SCID-HuPBL model of vaginal HIV transmission at nonpermeabilizing concentrations (24). Permeabilization and loss of viral core proteins greatly enhance the microbicide potential by causing irreversible virus inactivation.

ACKNOWLEDGMENTS

We thank Michelle Gignac for excellent technical assistance with the electron micrographs; Nicky Hoffman, Michael Piatak, and Jeff Lifson for SIV viral RNA analysis; Charla Henson for HIV viral RNA analysis; Julian Bess for providing virus for these studies; and Mike Grimes and Bill Bohn for the production of virus. Finally, we thank Lou Henderson, Zhaohao Liao, and David Ott for insightful suggestions on the manuscript.

This work was supported by grants to J.E.K.H. from the Public Health Service (AI31806, AI46291, and HD39613). This project was funded in part with funds from the NCI, under contract N01CO-12400.

REFERENCES

1. **Aloia, R. C., F. C. Jensen, C. C. Curtain, P. W. Mobley, and L. M. Gordon.** 1988. Lipid composition and fluidity of the human immunodeficiency virus. Proc. Natl. Acad. Sci. USA **85:**900–904.
2. **Arthur, L. O., J. W. Bess, Jr., E. N. Chertova, J. L. Rossio, M. T. Esser, R. E. Benveniste, L. E. Henderson, and J. D. Lifson.** 1998. Chemical inactivation of retroviral infectivity by targeting nucleocapsid protein zinc fingers: a candidate SIV vaccine. AIDS Res. Hum. Retrovir. **14:**S311–S319.
3. **Benveniste, R. E., D. Raben, R. W. Hill, W. B. Knott, J. E. Drummond, L. O. Arthur, P. B. Jahrling, W. R. Morton, L. E. Henderson, and G. Heidecker.** 1989. Molecular characterization and comparison of simian immunodeficiency virus isolates from macaques, mangabeys, and African green monkeys. J. Med. Primatol. **18:**287–303.
4. **Bess, J. W., Jr., R. J. Gorelick, W. J. Bosche, L. E. Henderson, and L. O. Arthur.** 1997. Microvesicles are a source of contaminating cellular proteins found in purified HIV-1 preparations. Virology **230:**134–144.
5. **Bess, J. W., Jr., P. J. Powell, H. J. Issaq, L. J. Schumack, M. K. Grimes, L. E. Henderson, and L. O. Arthur.** 1992. Tightly bound zinc in human immunodeficiency virus type 1, human T-cell leukemia virus type I, and other retroviruses. J. Virol. **66:**840–847.
6. **Brown, D.** 2002. Structure and function of membrane rafts. Int. J. Med. Microbiol. **291:**433–437.
7. **Brown, D. A., and E. London.** 2000. Structure and function of sphingolipid- and cholesterol-rich membrane rafts. J. Biol. Chem. **275:**17221–17224.
8. **Bukrinskaya, A., B. Brichacek, A. Mann, and M. Stevenson.** 1998. Establishment of a functional human immunodeficiency virus type 1 (HIV-1) reverse transcription complex involves the cytoskeleton. J. Exp. Med. **188:** 2113–2125.
9. **Campbell, S. M., S. M. Crowe, and J. Mak.** 2002. Virion-associated cholesterol is critical for the maintenance of HIV-1 structure and infectivity. AIDS **16:**2253–2261.
10. **Chertova, E., J. W. Bess, Jr., B. J. Crise, I. R. Sowder, T. M. Schaden, J. M. Hilburn, J. A. Hoxie, R. E. Benveniste, J. D. Lifson, L. E. Henderson, and L. O. Arthur.** 2002. Envelope glycoprotein incorporation, not shedding of surface envelope glycoprotein (gp120/SU), is the primary determinant of SU content of purified human immunodeficiency virus type 1 and simian immunodeficiency virus. J. Virol. **76:**5315–5325.
11. **Craven, R. C., A. E. Leure-duPree, R. A. Weldon, Jr., and J. W. Wills.** 1995. Genetic analysis of the major homology region of the Rous sarcoma virus Gag protein. J. Virol. **69:**4213–4227.
12. **Esser, M. T., D. R. Graham, L. V. Coren, C. M. Trubey, J. W. Bess, Jr., L. O. Arthur, D. E. Ott, and J. D. Lifson.** 2001. Differential incorporation of CD45, CD80 (B7-1), CD86 (B7-2), and major histocompatibility complex class I and II molecules into human immunodeficiency virus type 1 virions and microvesicles: implications for viral pathogenesis and immune regulation. J. Virol. **75:**6173–6182.
13. **Freed, E. O.** 2002. Viral late domains. J. Virol. **76:**4679–4687.
14. **Fuller, S. D., T. Wilk, B. E. Gowen, H. G. Krausslich, and V. M. Vogt.** 1997. Cryo-electron microscopy reveals ordered domains in the immature HIV-1 particle. Curr. Biol. **7:**729–738.
15. **Garrus, J. E., U. K. von Schwedler, O. W. Pornillos, S. G. Morham, K. H. Zavitz, H. E. Wang, D. A. Wettstein, K. M. Stray, M. Cote, R. L. Rich, D. G. Myszka, and W. I. Sundquist.** 2001. Tsg101 and the vacuolar protein sorting pathway are essential for HIV-1 budding. Cell **107:**55–65.
16. **Gonda, M. A., S. A. Aaronson, N. Ellmore, V. H. Zeve, and K. Nagashima.** 1976. Ultrastructural studies of surface features of human normal and tumor cells in tissue culture by scanning and transmission electron microscopy. J. Natl. Cancer Inst. **56:**245–263.
17. **Gordon, L. M., F. C. Jensen, C. C. Curtain, P. W. Mobley, and R. C. Aloia.** 1988. Thermotropic lipid phase separation in the human immunodeficiency virus. Biochim. Biophys. Acta **943:**331–342.
18. **Gottlinger, H. G., T. Dorfman, J. G. Sodroski, and W. A. Haseltine.** 1991. Effect of mutations affecting the p6 gag protein on human immunodeficiency virus particle release. Proc. Natl. Acad. Sci. USA **88:**3195–3199.
19. **Greene, W. C., and B. M. Peterlin.** 2002. Charting HIV's remarkable voyage through the cell: basic science as a passport to future therapy. Nat. Med. **8:**673–680.
20. **Guyader, M., E. Kiyokawa, L. Abrami, P. Turelli, and D. Trono.** 2002. Role for human immunodeficiency virus type 1 membrane cholesterol in viral internalization. J. Virol. **76:**10356–10364.
21. **Haynes, M. P., M. C. Phillips, and G. H. Rothblat.** 2000. Efflux of cholesterol from different cellular pools. Biochemistry **39:**4508–4517.
22. **Hermida-Matsumoto, L., and M. D. Resh.** 2000. Localization of human immunodeficiency virus type 1 Gag and Env at the plasma membrane by confocal imaging. J. Virol. **74:**8670–8679.
23. **Iyengar, S., J. E. Hildreth, and D. H. Schwartz.** 1998. Actin-dependent receptor colocalization required for human immunodeficiency virus entry into host cells. J. Virol. **72:**5251–5255.
24. **Khanna, K. V., K. J. Whaley, L. Zeitlin, T. R. Moench, K. Mehrazar, R. A. Cone, Z. Liao, J. E. Hildreth, T. E. Hoen, L. Shultz, and R. B. Markham.** 2002. Vaginal transmission of cell-associated HIV-1 in the mouse is blocked by a topical, membrane-modifying agent. J. Clin. Investig. **109:**205–211.
25. **Kilsdonk, E. P., P. G. Yancey, G. W. Stoudt, F. W. Bangerter, W. J. Johnson, M. C. Phillips, and G. H. Rothblat.** 1995. Cellular cholesterol efflux mediated by cyclodextrins. J. Biol. Chem. **270:**17250–17256.
26. **Kim, J. T., E. M. Kim, K. H. Lee, J. E. Choi, B. H. Jhun, and J. W. Kim.** 2002. Leucine zipper domain of HIV-1 gp41 interacted specifically with alpha-catenin. Biochem. Biophys. Res. Commun. **291:**1239–1244.
27. **Kozak, S. L., J. M. Heard, and D. Kabat.** 2002. Segregation of CD4 and CXCR4 into distinct lipid microdomains in T lymphocytes suggests a mechanism for membrane destabilization by human immunodeficiency virus. J. Virol. **76:**1802–1815.
28. **Leitinger, B., and N. Hogg.** 2002. The involvement of lipid rafts in the regulation of integrin function. J. Cell Sci. **115:**963–972.
29. **Liao, Z., L. M. Cimakasky, R. Hampton, D. H. Nguyen, and J. E. Hildreth.** 2001. Lipid rafts and HIV pathogenesis: host membrane cholesterol is required for infection by HIV type 1. AIDS Res. Hum. Retrovir. **17:**1009–1019.
30. **Lifson, J. D., J. L. Rossio, M. Piatak, Jr., T. Parks, L. Li, R. Kiser, V. Coalter, B. Fisher, B. M. Flynn, S. Czajak, V. M. Hirsch, K. A. Reimann, J. E. Schmitz, J. Ghrayeb, N. Bischofberger, M. A. Nowak, R. C. Desrosiers, and D. Wodarz.** 2001. Role of $CD8^+$ lymphocytes in control of simian immunodeficiency virus infection and resistance to rechallenge after transient early antiretroviral treatment. J. Virol. **75:**10187–10199.
31. **Lindwasser, O. W., and M. D. Resh.** 2001. Multimerization of human immunodeficiency virus type 1 Gag promotes its localization to barges, raft-like membrane microdomains. J. Virol. **75:**7913–7924.
32. **Liu, B., R. Dai, C. J. Tian, L. Dawson, R. Gorelick, and X. F. Yu.** 1999. Interaction of the human immunodeficiency virus type 1 nucleocapsid with actin. J. Virol. **73:**2901–2908.
33. **London, E., and D. A. Brown.** 2000. Insolubility of lipids in triton X-100: physical origin and relationship to sphingolipid/cholesterol membrane domains (rafts). Biochim. Biophys. Acta **1508:**182–195.
34. **Lub, M., Y. van Kooyk, S. J. van Vliet, and C. G. Figdor.** 1997. Dual role of the actin cytoskeleton in regulating cell adhesion mediated by the integrin lymphocyte function-associated molecule-1. Mol. Biol. Cell **8:**341–351.
35. **Luftig, R. B., and L. D. Lupo.** 1994. Viral interactions with the host-cell cytoskeleton: the role of retroviral proteases. Trends Microbiol. **2:**178–182.
36. **Nakamura, M., H. Okada, H. Sasaki, K. Yoshida, M. Kamada, N. Okada, M. Terada, and T. Ohno.** 1996. Quantification of the CD55 and CD59, mem-

brane inhibitors of complement on HIV-1 particles as a function of complement-mediated virolysis. Microbiol. Immunol. **40:**561–567.
37. **Nguyen, D. H., and J. E. Hildreth.** 2000. Evidence for budding of human immunodeficiency virus type 1 selectively from glycolipid-enriched membrane lipid rafts. J. Virol. **74:**3264–3272.
38. **Nguyen, D. H., Z. Liao, J. T. Buckley, and J. E. Hildreth.** 1999. The channel-forming toxin aerolysin neutralizes human immunodeficiency virus type 1. Mol. Microbiol. **33:**659–666.
39. **Nguyen, D. H., and D. Taub.** 2002. CXCR4 function requires membrane cholesterol: implications for HIV infection. J. Immunol. **168:**4121–4126.
40. **Ono, A., and E. O. Freed.** 2001. Plasma membrane rafts play a critical role in HIV-1 assembly and release. Proc. Natl. Acad. Sci. USA **98:**13925–13930.
41. **Orentas, R. J., and J. E. Hildreth.** 1993. Association of host cell surface adhesion receptors and other membrane proteins with HIV and SIV. AIDS Res. Hum. Retrovir. **9:**1157–1165.
42. **Ott, D. E.** 1997. Cellular proteins in HIV virions. Rev. Med. Virol. **7:**167–180.
43. **Ott, D. E., L. V. Coren, D. G. Johnson, B. P. Kane, R. C. Sowder II, Y. D. Kim, R. J. Fisher, X. Z. Zhou, K. P. Lu, and L. E. Henderson.** 2000. Actin-binding cellular proteins inside human immunodeficiency virus type 1. Virology **266:**42–51.
44. **Ott, D. E., L. V. Coren, B. P. Kane, L. K. Busch, D. G. Johnson, R. C. Sowder II, E. N. Chertova, L. O. Arthur, and L. E. Henderson.** 1996. Cytoskeletal proteins inside human immunodeficiency virus type 1 virions. J. Virol. **70:**7734–7743.
45. **Ott, D. E., S. M. Nigida, Jr., L. E. Henderson, and L. O. Arthur.** 1995. The majority of cells are superinfected in a cloned cell line that produces high levels of human immunodeficiency virus type 1 strain MN. J. Virol. **69:**2443–2450.
46. **Palmer, E., M. L. Martin, C. Goldsmith, and W. Switzer.** 1988. Ultrastructure of human immunodeficiency virus type 2. J. Gen. Virol. **69:**1425–1429.
47. **Popik, W., T. M. Alce, and W. C. Au.** 2002. Human immunodeficiency virus type 1 uses lipid raft-colocalized CD4 and chemokine receptors for productive entry into $CD4^+$ T cells. J. Virol. **76:**4709–4722.
48. **Reed, L. J., and H. Muench.** 1938. A simple method of estimating fifty percent endpoints. Am. J. Hyg. **27:**493–497.
49. **Rey, O., J. Canon, and P. Krogstad.** 1996. HIV-1 Gag protein associates with F-actin present in microfilaments. Virology **220:**530–534.
50. **Roos, J. W., M. F. Maughan, Z. Liao, J. E. Hildreth, and J. E. Clements.** 2000. LuSIV cells: a reporter cell line for the detection and quantitation of a single cycle of HIV and SIV replication. Virology **273:**307–315.
51. **Rossio, J. L., M. T. Esser, K. Suryanarayana, D. K. Schneider, J. W. Bess, Jr., G. M. Vasquez, T. A. Wiltrout, E. Chertova, M. K. Grimes, Q. Sattentau, L. O. Arthur, L. E. Henderson, and J. D. Lifson.** 1998. Inactivation of human immunodeficiency virus type 1 infectivity with preservation of conformational and functional integrity of virion surface proteins. J. Virol. **72:**7992–8001.
52. **Sasaki, H., M. Nakamura, T. Ohno, Y. Matsuda, Y. Yuda, and Y. Nonomura.** 1995. Myosin-actin interaction plays an important role in human immunodeficiency virus type 1 release from host cells. Proc. Natl. Acad. Sci. USA **92:**2026–2030.
53. **Shoeman, R. L., C. Kesselmier, E. Mothes, B. Honer, and P. Traub.** 1991. Non-viral cellular substrates for human immunodeficiency virus type 1 protease. FEBS Lett. **278:**199–203.
54. **Shoeman, R. L., C. Sachse, B. Honer, E. Mothes, M. Kaufmann, and P. Traub.** 1993. Cleavage of human and mouse cytoskeletal and sarcomeric proteins by human immunodeficiency virus type 1 protease: actin, desmin, myosin, and tropomyosin. Am. J. Pathol. **142:**221–230.
55. **Suryanarayana, K., T. A. Wiltrout, G. M. Vasquez, V. M. Hirsch, and J. D. Lifson.** 1998. Plasma SIV RNA viral load determination by real-time quantification of product generation in reverse transcriptase-polymerase chain reaction. AIDS Res. Hum. Retrovir. **14:**183–189.
56. **Tomasselli, A. G., J. O. Hui, L. Adams, J. Chosay, D. Lowery, B. Greenberg, A. Yem, M. R. Deibel, H. Zurcher-Neely, and R. L. Heinrikson.** 1991. Actin, troponin C, Alzheimer amyloid precursor protein and pro-interleukin 1β as substrates of the protease from human immunodeficiency virus. J. Biol. Chem. **266:**14548–14553.
57. **Viard, M., I. Parolini, M. Sargiacomo, K. Fecchi, C. Ramoni, S. Ablan, F. W. Ruscetti, J. M. Wang, and R. Blumenthal.** 2002. Role of cholesterol in human immunodeficiency virus type 1 envelope protein-mediated fusion with host cells. J. Virol. **76:**11584–11595.
58. **Wilk, T., B. Gowen, and S. D. Fuller.** 1999. Actin associates with the nucleocapsid domain of the human immunodeficiency virus Gag polyprotein. J. Virol. **73:**1931–1940.
59. **Yancey, P. G., W. V. Rodrigueza, E. P. Kilsdonk, G. W. Stoudt, W. J. Johnson, M. C. Phillips, and G. H. Rothblat.** 1996. Cellular cholesterol efflux mediated by cyclodextrins: demonstration of kinetic pools and mechanism of efflux. J. Biol. Chem. **271:**16026–16034.
60. **Yong, W. H., S. Wyman, and J. A. Levy.** 1990. Optimal conditions for synthesizing complementary DNA in the HIV-1 endogenous reverse transcriptase reaction. AIDS **4:**199–206.
61. **Zhang, H., G. Dornadula, and R. J. Pomerantz.** 1996. Endogenous reverse transcription of human immunodeficiency virus type 1 in physiological microenviroments: an important stage for viral infection of nondividing cells. J. Virol. **70:**2809–2824.
62. **Zhang, H., L. Wang, S. Kao, I. P. Whitehead, M. J. Hart, B. Liu, K. Duus, K. Burridge, C. J. Der, and L. Su.** 1999. Functional interaction between the cytoplasmic leucine-zipper domain of HIV-1 gp41 and p115-RhoGEF. Curr. Biol. **9:**1271–1274.